



1 Validating Plutonium-239+240 as novel soil redistribution tracer - a
2 comparison to measured sediment yield

3 Katrin Meusburger^{1*}, Paolo Porto², Judith Kobler Waldis³, Christine Alewell³

4

5 ¹Swiss Federal Institute for Forest, Snow and Landscape Research WSL, CH-8903, Birmensdorf,
6 Switzerland

7 ²Dipartimento di Agraria, Università degli Studi Mediterranea di Reggio Calabria, Reggio Calabria,
8 Italy

9 ³Environmental Geosciences, University of Basel, Switzerland

10

11 *corresponding author: katrin.meusburger@wsl.ch

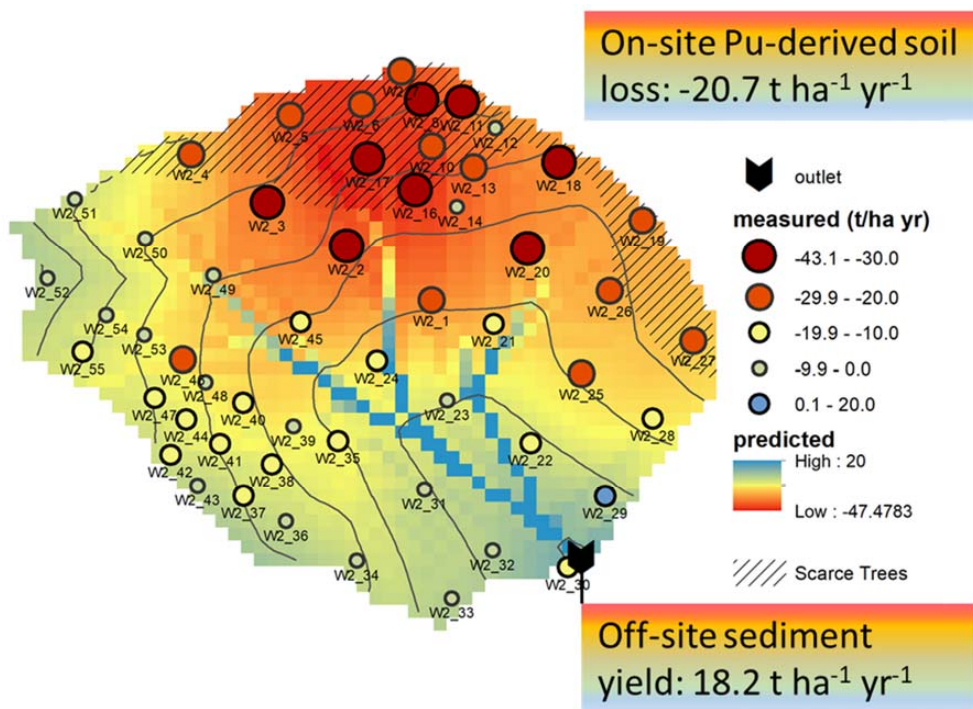
12



13 **Abstract**

14 Quantifying soil redistribution rates is a global challenge addressed with direct sediment measurements
15 (e.g., traps), models and isotopic, geochemical and radiogenic tracers. The isotope of Plutonium, namely
16 Pu-239+240, is a relatively new soil redistribution tracer in this challenge. Direct validation of Pu-
17 239+240 as soil redistribution is, however, still missing. We used a unique sediment yield time series
18 in Southern Italy, reaching back to the initial fallout of Pu-239+240 to verify Pu-239+240 as a soil
19 redistribution tracer. Distributed soil samples (n=55) were collected in the catchment, and at potential
20 undisturbed reference sites (n=22), Pu-239+240 was extracted, measured with ICP-MS and converted
21 to soil redistribution rates. Finally, we used a Generalized Additive model (GAM) to regionalize soil
22 redistribution estimates for the catchment. For the catchment sites, mean Pu-239+240 inventories were
23 significantly reduced ($16.8 \pm 10.2 \text{ Bq m}^{-2}$) compared to the reference inventory ($40.5 \pm 3.5 \text{ Bq m}^{-2}$)
24 indicating the dominance of erosion. Converting these inventory losses into soil erosion rates resulted
25 in an average soil loss of $22.2 \pm \text{SD } 7.2 \text{ t ha}^{-1} \text{ yr}^{-1}$. The uncertainties of the approach stemmed mainly
26 from the high measurement uncertainties of low-activity samples where samples have been bulked over
27 depth. Therefore, we recommend taking incremental soil samples and extracting ~20g of soil. The
28 geographic coordinates and the flow accumulation best described the spatial pattern of erosion rates in
29 the GAM model. Using those predictors to upscale Pu-derived soil redistribution rates for the entire
30 catchment resulted in an average on-site loss of $20.7 \text{ t ha}^{-1} \text{ yr}^{-1}$, which corresponds very well to the long-
31 term average sediment yield of $18.7 \text{ t ha}^{-1} \text{ yr}^{-1}$ measured at the catchment outlet and to Cs-137 derived
32 soil redistribution rates. Overall, this comparison of Pu-derived soil redistribution rates with measured
33 sediment yield data validates Pu-239+240 as a suitable retrospective soil redistribution tracer.

34 **Graphical abstract**



35

36



37 **1 Introduction**

38 Soil erosion endangers climate and food security and has considerable adverse off-site effects on
39 freshwater systems (Reichstein et al., 2013; Amundson et al., 2015; Alewell et al., 2016; Panagos et al.,
40 2016; Borrelli et al., 2017; Alewell et al., 2020). Plutonium isotopes, with their previous hazardous
41 impacts on the environment and released as a product of thermonuclear weapons testing and from
42 nuclear accidents (e.g. Chernobyl), may serve as a tool to quantify long-term soil loss (Alewell et al.,
43 2017).

44 The approach to use Pu-239+240 as soil and sediment tracer is parallel to other fallout radionuclides
45 (FRN) (Xu et al., 2015; Meusburger et al., 2018). Once deposited on the ground, FRNs strongly bind
46 to soil particles and move across the landscape primarily through physical soil redistribution processes
47 (IAEA, 2014). In this way, fallout radionuclides provide an effective and retrospective (since the time
48 of the fallout) track of net soil and sediment redistribution (Zapata, 2003). However, Cs-137, the most
49 commonly applied soil redistribution tracer, will reach its detection limit soon due to the successive
50 decay (half-life = 30.17 years). Thus, alternative tracers like excess Pb-210 and Pu-239+240 have been
51 explored (Wallbrink and Murray, 1996; Matisoff et al., 2002; Mabit et al., 2008; Kato et al., 2010; Porto
52 et al., 2013; Teramage et al., 2015; Xu et al., 2015; Meusburger et al., 2018). While Pb-210 is associated
53 with high uncertainties (Porto and Walling, 2012; Mabit et al., 2014; Meusburger et al., 2018), the
54 characteristics of Pu-239+240 seem more promising for soil tracing (Alewell et al., 2017).

55 The advent of Pu-239+240 as a soil redistribution tracer was accelerated by the adoption of the less
56 time-consuming (minutes instead of hours per sample) Inductively Coupled Plasma Mass spectrometry
57 (ICP-MS). It was a door opener for using Pu-239+240 as a soil erosion tracer. The application of Pu-
58 239+240 comes along with other advantages, such as i) reduced initial spatial variability at undisturbed,
59 so-called reference sites (Alewell et al., 2014; Meusburger et al., 2016), ii) less preferential uptake by
60 plants (Froehlich et al., 2016), iii) the possibility to assess the origin of the fallout by determining ^{240}Pu
61 to ^{239}Pu atom ratios or Cs-137 to Pu-239+240 activity ratios (Ketterer et al., 2004; Xu et al., 2013;
62 Meusburger et al., 2016; Meusburger et al., 2020), iv) considerably smaller soil sample volume needed
63 for analysis, and v) no decline due to decay, which is of particular relevance for locations with low
64 initial Cs-137 fallout such as the southern hemisphere (Tims et al., 2010). The potential of Pu-239+240
65 further convenes with the availability of the new conversion model "Modelling Deposition and Erosion
66 rates with RadioNuclides (MODERN)", suitable for estimating soil redistribution rates by comparing
67 reference with soil redistribution affected inventories with any FRN (Arata et al., 2016a; Arata et al.,
68 2016b).

69 Several studies (Schimmack et al., 2001; Tims et al., 2010; Hoo et al., 2011; Lal et al., 2013; Michelotti
70 et al., 2013; Xu et al., 2013; Xu et al., 2015; Meusburger et al., 2018) have highlighted $^{239+240}\text{Pu}$'s
71 suitability as a soil redistribution tracer. However, to date, direct validation efforts to compare on-site
72 FRN-based soil erosion rates with off-site sediment yields have focused on other FRNs such as Cs-137

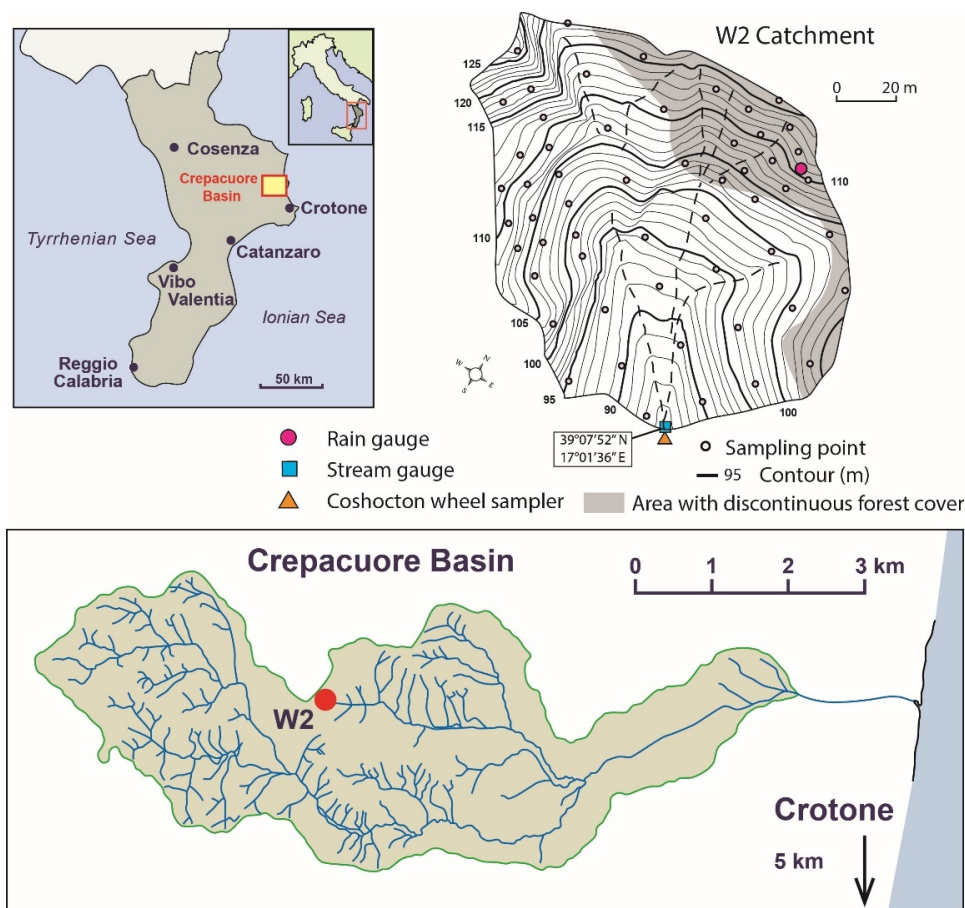


73 and excess ^{210}Pb (Porto et al., 2001; Porto et al., 2003; Porto and Walling, 2012; Porto and Callegari,
74 2022). For $^{239+240}\text{Pu}$ -derived soil redistribution rates, such a direct validation is not achieved yet, to the
75 best of our knowledge. This study aims to fill this gap by validating $^{239+240}\text{Pu}$ -derived soil redistribution
76 rates with a long-term time series of measured catchment suspended sediment yields.

77 **2 Materials and Methods**

78 **2.1 Study site and soil sampling**

79 This study takes advantage of a unique long-term sediment yield monitoring catchment (W2, 1.38 ha)
80 located near Crotona in Calabria, Southern Italy (35 m a.s.l., 39°09'02"N, 17°08'10"E). The steep
81 catchment with a mean average slope of ca. 35% is located in the ephemeral headwaters of the larger
82 Crepacuore basin (Fig. 1). The geology of this area consists of Upper Pliocene and Quaternary materials
83 and produced soils with a clay loam texture with 14.6%, 49.2%, and 36.2% of sand, silt, and clay,
84 respectively. The catchment was never ploughed, but in 1968, *Eucalyptus occidentalis* Engl. was
85 planted and cut again in 1978 and 1990. The tree cover is partly patchy, with about 20% of the area on
86 south-facing slopes having discontinuous tree and grass cover. The climate is Mediterranean, with a
87 mean annual precipitation of ~670 mm, predominantly occurring from October to March.



88

89 Fig. 1 Location of the studied headwater catchment W2 within the Crepacuore Basin (lower panel
90 indicated by a red dot), Calabria, Italy.

91 In 2014, the collection of soil samples in the catchment was undertaken along an approximate 20 m ×
92 20 m grid with additional cores collected from areas characterized by marked variability of vegetation
93 cover or topography (Fig. 1). The samples were taken with a steel core tube (10 cm diameter) driven
94 into the ground to a depth of 15 cm by a motorized percussion corer and subsequently extracted using
95 a hand-operated winch. For each sampling point, two cores were taken, and they were bulked before
96 analysis. This procedure provided a total of 55 composite bulk cores over the catchment area.

97 In March 2021, a new sampling campaign was undertaken to obtain information at the reference area
98 to establish the baseline for $^{239+240}\text{Pu}$ in the area. In this case, three depth profiles and nineteen additional
99 bulk reference soil cores were collected in adjacent undisturbed rangeland with some scattered oaks
100 (*Quercus pubescens*) at a similar altitude to the study catchment (see Porto and Callegari, 2022). The
101 samples were collected using the same sampling device consisting of a motorized soil column cylinder



102 auger set in which a core tube (60 cm in length) with a larger internal diameter (11 cm) is
103 accommodated. The three depth profiles were sectioned into increments of 2 cm and were analyzed
104 separately for ^{137}Cs and $^{239+240}\text{Pu}$ content. Before radiometric analyses, all samples were dried and sieved
105 to <2 mm. In a previous study, the soil samples collected within the catchment were analyzed for Cs-
106 137 using high-resolution HPGe detectors available at the Agraria Department at the University
107 Mediterranea of Reggio Calabria, Italy (Porto et al., 2014). Counting times for the samples collected
108 during that campaign were ca. 80,000 s, providing a precision of ca. $\pm 10\%$ at the 95% confidence level.
109 The reference samples of 2021 were also analyzed for Cs-137 with the same detector settings. All Cs-
110 137 measurements were decay corrected to 01.01.2014 and used to calculate Pu-239+240 to Cs-137
111 activity ratios.

112 **2.2 Extraction of Pu-239+240 and mass spectrometry for atom ratio and concentration** 113 **measurements**

114 All samples (5-10g) were oven-dried at 105°C for 48 h, mechanically disaggregated and dry-sieved to
115 recover the <2 mm fraction. First, a representative sub-sample of this fraction was spiked with ~ 0.005
116 Bq of a ^{242}Pu yield tracer (licensed solution from NIST). Next, Pu was leached with 16M nitric acid
117 overnight at 80°C and separated from the leach solution using a Pu-selective TEVA resin (Ketterer et
118 al., 2011). The isotope dilution calculations determined the masses of ^{239}Pu and ^{240}Pu present in the
119 sample and then converted them into the summed Pu-239+240 activity. The analysis was done with a
120 Thermo X7 quadrupole ICP-MS system at Universidad de Cádiz. Please refer to Meusburger et al.
121 (2020) for details on the instrument method.

122 **2.3 Conversion of Pu-239+240 activities to soil redistribution rates**

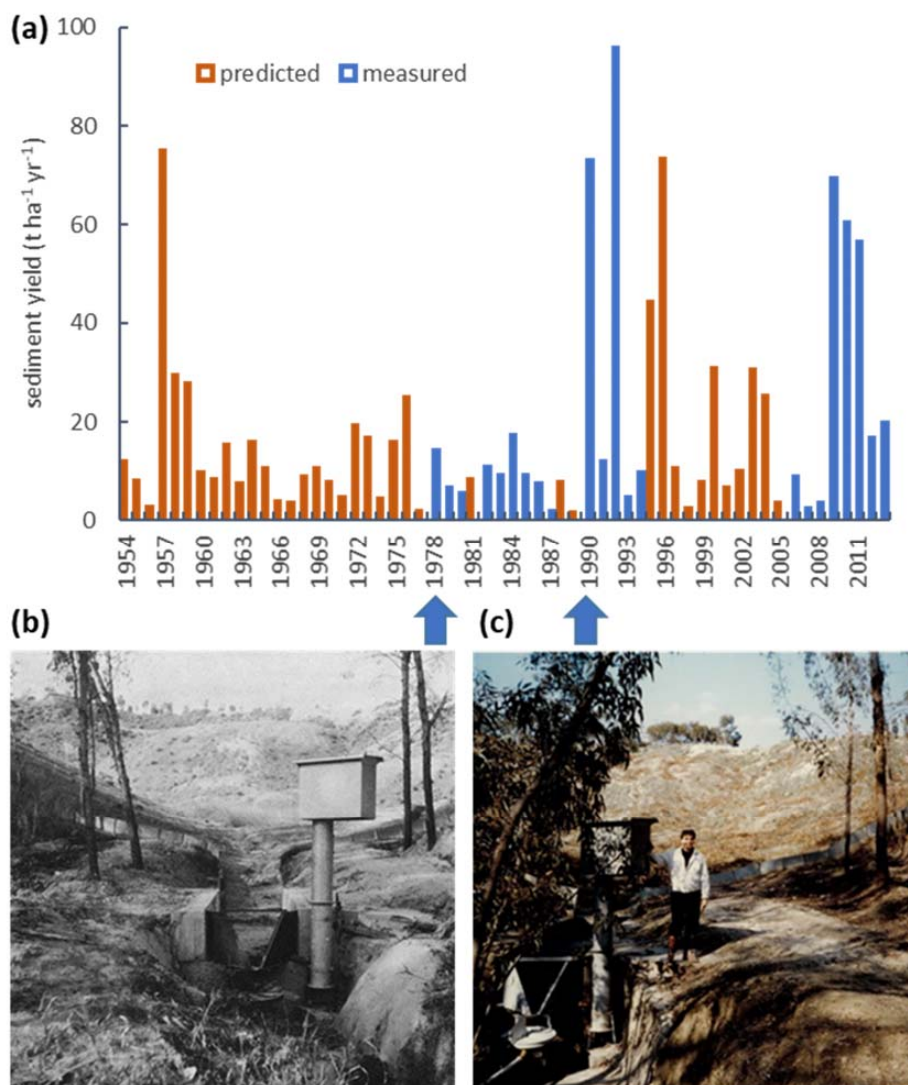
123 The total inventory (Bq m^{-2}) of each bulk soil core was calculated as the product of the measured Pu-
124 239+240 activity (Bq kg^{-1}) and the dry mass of the <2 mm fraction of the bulk core (kg), divided by the
125 surface area associated with the soil core (m^2). The inventories were converted into soil redistribution
126 rates using the Profile Distribution model PDM (Walling et al., 2002; Walling et al., 2014) and the
127 model Modelling Deposition and Erosion rates with RadioNuclides (MODERN (Arata et al., 2016a;
128 Arata et al., 2016b)). The profile distribution model is commonly employed to interpret the shape of an
129 FRN along the soil profile. It assumes an exponential depth distribution, and the depth of soil removed
130 by erosion is estimated by comparing the reduction in the FRN inventory with that related to the
131 reference site (see Porto et al., 2003). MODERN aligns the sampling site's total inventory to the
132 measured shape of the reference site's depth profile to estimate the thickness of soil losses/gains. The
133 intersection along the soil profile represents the solution of the model. We accounted for the uncertainty
134 in the conversion procedure by running both conversion models 100 times, sampling from the reference
135 and the erosion inventory within the uncertainty bounds and for the PDM in addition to the shape factor



136 h_0 . The sampling was done from normal distributions, defined by the mean measured value and the
137 standard deviations (SD): i) of the repeated ICP-MS measurements for the erosional sites, ii) of the
138 replicate reference inventories, iii) of the three depth profiles for the h_0 factor (Supplementary Figure
139 1).

140 **2.4 Sediment yield measurements**

141 Since 1978, precipitation, runoff and sediment yield have been measured in the W2 catchment (Cantore
142 et al., 1994). Precipitation was recorded using a tipping bucket rain gauge, and runoff was measured at
143 the outlet using an H-flume structure equipped with a mechanical stage recorder. Below the H-flume,
144 the sediment load was measured with a Coshocton wheel sampler (Porto et al., 2003). Sediment yield
145 data used in this analysis is related to the period from 1978 to 1994 (Cantore et al., 1994) and from 2006
146 to 2013 (Fig. 2). However, due to the malfunctioning of the sediment sampling equipment in the
147 catchment during some events, direct measurements of total annual sediment yield values are not
148 available for all years. To account for these missing years, the corresponding sediment output was
149 estimated using the Arnoldus Index, for which long-term observations are available from the station of
150 Crotone located ca. 10 km distant from the study catchment (see Capra et al., 2017). These estimates
151 were then incorporated into the annual record of sediment yield (Fig. 2), and the sediment yield data
152 was extrapolated to cover the period 1963–2013, corresponding to the period captured by Pu-239+240
153 derived soil redistribution assessments.



154

155 Fig. 2 Measured (orange) and predicted (blue) annual sediment yield (t ha⁻¹ yr⁻¹) of the headwater
156 catchment W2 (a). Predictions of sediment yields are based on a significant relation to Arnoulds
157 erosivity index. In 1968, *Eucalyptus occidentalis* Engl. was planted in the catchment that was harvested
158 in 1978 (b) (photo by M. Raglione, from Avolio et al., (1980)) and a second time in 1990 (c).

159 2.5 Spatial extrapolation of Pu-239+240 derived estimates

160 Regionalization of the point erosion estimates was done to compare the sediment yields measured at
161 the catchment's outlet with Pu-derived sediment yields. Therefore, generalized additive models (GAM)
162 were fitted to the measured erosion estimates. GAMs can account for nonlinear relationships by
163 coefficients that can be expanded as smooth functions of covariates. The smooth terms were modelled



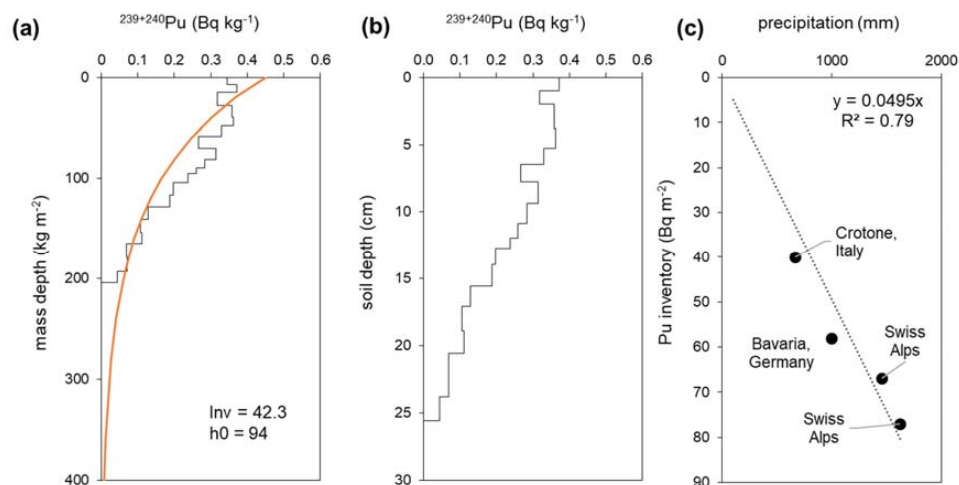
164 by splines, and geographic coordinates (x and y) were modelled as a 2d spline. To prevent overfitting,
165 we used the restricted maximum likelihood (REML) method with the R package mgcv (Wood, 2006).
166 As spatial covariates, elevation, slope, aspect, flow accumulation, and scarce, discontinuous tree cover
167 (as 0 and 1 categorical variables, see Fig. 1) were tested. These covariates were derived from a DEM
168 with 3m spatial resolution using the terrain function from the raster package. Because of the small
169 sample size of 55 sites, only a maximum of three covariables could be added to the model. For cross-
170 validation (n=50) of the spatial prediction, the data were randomly split into 80% training and 20%
171 testing data.

172 **3 Results and Discussion**

173 **3.1 Pu-239+240 distribution at the reference sites**

174 The mean measured ^{240}Pu to ^{239}Pu atom ratios at the reference and sampling sites were 0.179 ± 0.03 .
175 These atom ratios corresponded to the atom ratio found for the global fallout (Kelley et al., 1999) and
176 confirmed global fallout as the sole source of Pu in the catchment.

177 The three reference depth profiles Pu-239+240 activity at the reference site showed different shapes
178 with soil depth (Supplementary Figure 1). While profile 2 displays the expected exponential decline
179 with soil depth, profile 1 shows signs typically expected from erosional processes and profile 3 of
180 depositional processes (Supplementary Figure 1). Therefore, only profile 2 was assessed to be suitable
181 for extracting the shape of the depth distribution for the conversion procedure (Fig. 3a). The penetration
182 depth of Pu-239+240 reached 205 kg m^{-2} , corresponding to 26 cm soil depth (Fig. 3b). With an
183 exponential model fit of the PDM, we derived an h_0 at 94 kg m^{-2} , representing the point where half of
184 the activity is stored. The mean Pu-239+240 reference inventory was estimated at $42.3 \pm 3.5 \text{ Bq m}^{-2}$.
185 The fitted surface soil (0 cm) concentration was 0.45 Bq kg^{-1} (Fig. 3a).



186

187 Fig. 3 (a) Pu-239+240 activity with soil mass depth measured at the reference site (selected profile 2).
188 Inv corresponds to the total inventory of the soil, and h_0 to the shape factor of the exponential fit
189 (orange). (b) Pu-239+240 activity with soil depth (cm). (c) Relation between Pu reference inventories
190 and precipitation for studies in the Alps, Southern Germany (Schimmack et al., 2001; Alewell et al.,
191 2014; Meusburger et al., 2018).

192 The Pu-239+240 measurements of the 19 bulk reference soil cores showed a bimodal distribution with
193 six high inventories clustering at a mean of $40.2 \pm 4.4 \text{ Bq m}^{-2}$ and 13 low inventories of $15.0 \pm 2.8 \text{ Bq}$
194 m^{-2} . The Pu-239+240 activities of the bulk soil cores with low inventories had values $<0.043 \text{ Bq kg}^{-1}$,
195 close to the detection limit, and the standard deviation of replicate measurement of these samples was
196 high. To verify the plausibility of these low inventories, we calculated the Pu to Cs activity ratios. For
197 European soil samples, the activity ratio of Pu to Cs (with Cs being decay corrected to 2014) is expected
198 between 81 and 24 (Meusburger et al., 2020). However, the low inventory bulk cores had mean Pu/Cs
199 ratios of 156, which is clearly outside this range. A possible explanation for these very low Pu values
200 in the reference site might be due to the mixing and dilution of deeper layers with no Pu activity into
201 the bulk reference soil cores. Therefore, these low reference bulk samples were removed from further
202 analysis. Bulking of Pu samples causing a dilution of the Pu activity should be avoided, particularly in
203 areas of high erosion or low initial fallout (Wilken et al., 2021). Here, we were able to resolve the
204 dilution problem due to the availability of Cs-137 data, as the Cs-137 to Pu-239+240 activity ratios
205 were valuable in identifying the suitability of the reference samples. The plausibility of the Pu inventory
206 was further underpinned when the inventory was related to the mean annual precipitation of other
207 published European studies (Fig. 3c). The few published Pu inventories in Europe (Schimmack et al.,
208 2001; Alewell et al., 2014; Meusburger et al., 2018) show a linear relation to mean annual precipitation
209 with 77, 67, 58 Bq m^{-2} for 1650, 1450, 950 mm of rainfall. The high inventory of this study of 40.2 Bq
210 m^{-2} plots on the linear relation (Fig. 3c), while the low inventory of 15 Bq m^{-2} is below the expected



211 amount given the catchment's mean annual precipitation. Taking the depth distribution reference and
212 only the six high inventories of bulk soil cores into account, the mean reference inventory of the soil
213 profiles was $40.5 \pm 3.5 \text{ Bq m}^{-2}$ with a coefficient of variation of 8.6%.

214 All in all, following the above-described procedure, the Pu-239+240 reference inventories had a small
215 spatial variability with a CV of <9%. For Cs-137, the CV was 11.6% in the same reference area (see
216 Porto and Callegari, 2022). The spatial variability of Pu in reference sites was comparable to previous
217 studies (Alewell et al., 2014; Meusburger et al., 2016).

218 **3.2 Catchment inventories and soil redistribution rates at sampling points**

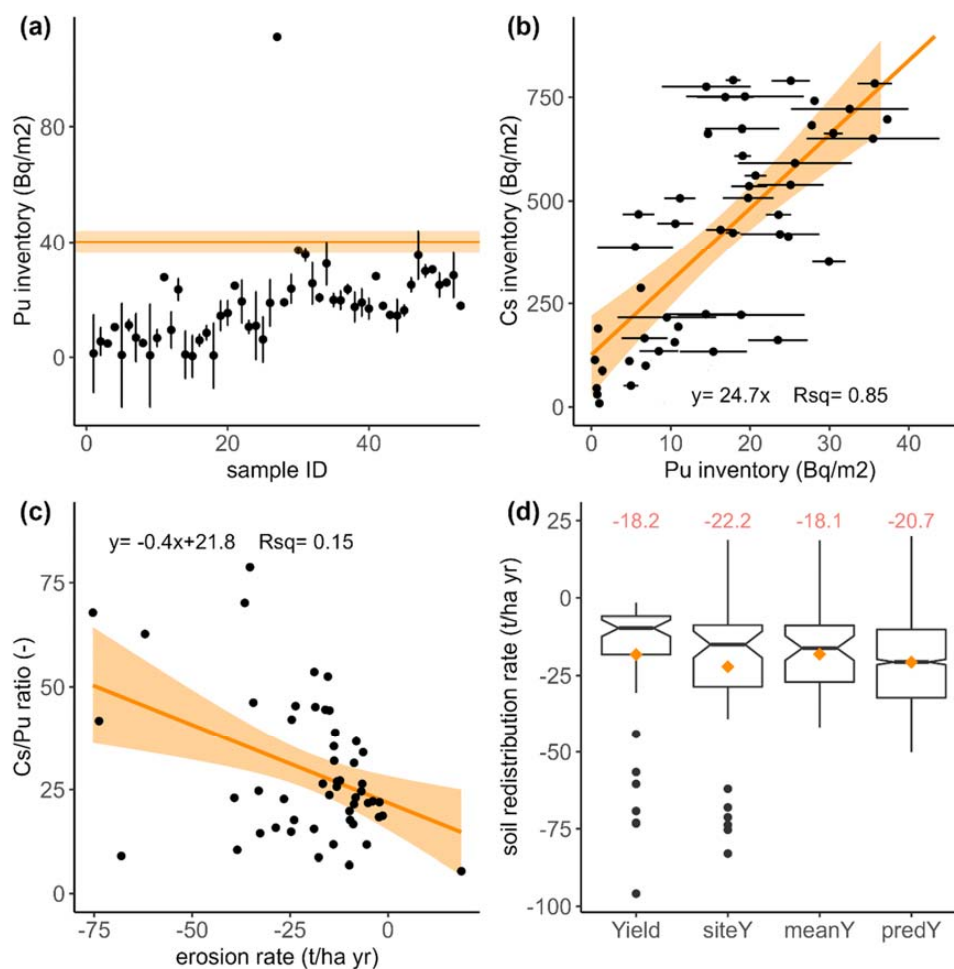
219 The Pu-239+240 activities at the sampling sites ranged from 0.001 to 0.143 Bq kg^{-1} with a mean of
220 0.066 Bq kg^{-1} . The uncertainties of repeated ICP-MS measurements increase with decreasing activities
221 from the smallest SD of $0.0004 \text{ Bq kg}^{-1}$ to the largest of 0.067 Bq kg^{-1} corresponding to <1% to larger
222 >100% of the measured activity with a median of 20%.

223 The respective mean Pu-239+240 inventories for all 55 sites were 16.8 Bq m^{-2} with a spatial SD of
224 $\pm 10.2 \text{ Bq m}^{-2}$, thus less than half of the reference inventory. Given the uncertainty bounds, all
225 inventories, except for four sites, were significantly smaller than the reference inventory, indicating soil
226 erosion (Fig. 4a). One site close to the catchment outlet had a very high Pu-239+240 inventory of 111
227 Bq m^{-2} exceeding the reference inventory by almost three times (Fig. 4a). The Pu-239+240 inventories
228 are significantly ($p < 0.001$) correlated to the Cs-137 inventories with 24.7 times more Bq m^{-2} for Cs-
229 137 (Fig. 4b). The Cs/Pu activity ratios of the catchment sites were at the lower range of the plausible
230 fallout range (between 23.9 = global and 81.3 = Chernobyl) with a mean value of 24.7. The activity
231 ratios are significantly ($p < 0.005$) decreasing with decreasing erosion rates even though R_{sq} of the
232 regression is with 0.15 very low (Fig. 4c).

233 This depletion in Cs-137 pointed towards a preferential loss of Cs-137 during soil loss. A possible
234 explanation might be that Cs-137 is transported with different soil particles as Pu, which are more
235 susceptible to soil erosion. It is known that Pu-239+240 exhibits a different sorption behaviour to soil
236 particles compared to, e.g. Cs-137. Pu is mainly associated with organic matter and sesquioxides in
237 addition to clay particles, whereas Cs-137 is predominantly bound to the fine mineral clay fraction
238 (Lujanienė et al., 2002; Qiao et al., 2012; Meusburger et al., 2016; Xu et al., 2017). As a consequence,
239 Pu-239+240 is more exchangeable and might more easily migrate downward in soils (Schimmack et
240 al., 2001; Meusburger et al., 2016). This different sorption behaviour may result in different depth
241 distributions, which have important implications for its use as a soil erosion tracer, e.g. regarding the
242 conversion of measured FRN inventory changes into soil redistribution rates. Further, it may also have
243 implications regarding interpreting Cs-137 to Pu-239+240 activity ratios that may be shifted outside the
244 expected ranges at sites affected by soil redistribution.



245



246

247 Fig. 4 (a) Pu-239+240 inventories with measurement errors in relation to sample ID (points) and the
248 reference inventory (orange line with ribbon). (b) Relation between Pu-239+240 and Cs-137 inventories
249 (error bars indicate the measurement error for Pu) with a linear trend line. (c) Activity ratio of Cs to Pu
250 versus erosion rate. (d) Measured sediment yield at catchment outlet (Yield), Pu-derived erosion rates
251 based on measured inventories within the catchment (siteY) and as a mean of the repeated conversion
252 results (meanY), and mean of regionalized catchment Pu-derived erosion rates (predY). Orange points
253 and text show the mean values of each approach.

254 3.3 Comparison of Pu-239+240 derived soil redistribution rates and sediment yield of 255 the catchment

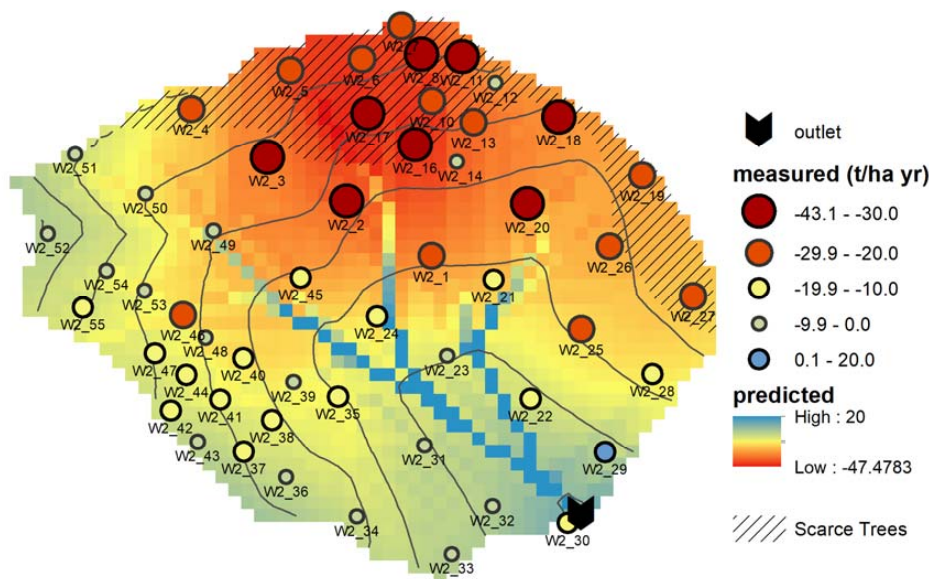
256 We produced three sets of Pu-derived soil redistribution rates using i) direct conversion of the site
257 inventories (siteY) and ii) the average of 100 Monte Carlo conversion models per site generated by
258 sampling within the uncertainty ranges of all input parameters (meanY) and iii) regionalized estimates



259 for the catchment (predY). For the point estimates will refer to these meanY in the following because
260 the uncertainty related to the entire procedure is included in this second set of redistribution rates.

261 Soil redistribution rates were highly variable within the catchment (Fig. 5). The highest soil loss with
262 $43 \pm 20 \text{ t ha}^{-1} \text{ yr}^{-1}$ occurred in the upper part with patchy tree cover. Generally, the sites with scarce tree
263 cover and adjacent sites showed the highest soil erosion rates. Downslope and towards the outlet of the
264 catchment, the erosion rates decrease. Close to the outlet, soil deposition of $18.7 \pm 2.0 \text{ t ha}^{-1} \text{ yr}^{-1}$ was
265 observed in one measurement point (W2_29). The deposition rate is, however, difficult to quantify
266 without knowledge of the respective soil source area or a Pu depth profile in the deposition site. The
267 average of all measured site redistribution rates (siteY) indicated erosion of $-22.2 \text{ t ha}^{-1} \text{ yr}^{-1}$ with a spatial
268 standard deviation of $\pm 21.1 \text{ t ha}^{-1} \text{ yr}^{-1}$. On average, the standard deviation, derived from repeated Monte
269 Carlo conversions, of these redistribution rates were $7.2 \text{ t ha}^{-1} \text{ yr}^{-1}$, with a slightly lower median of the
270 standard deviations of $4.2 \text{ t ha}^{-1} \text{ yr}^{-1}$ corresponding to a mean CV of 45% and a median CV of 36%.
271 Generally, higher erosion estimates are subject to higher standard deviations resulting from higher
272 uncertainties for measuring low Pu activities. Excluding these measurement uncertainties from the
273 Monte Carlo conversion reduced the CV of the erosion estimates to mean and median CVs of 19% and
274 13%, respectively.

275 The XY-coordinates, elevation, and flow accumulation best explained the spatial pattern of soil
276 redistribution rates. The deviance explained with these two spatial covariates was 56.7%, with lower
277 accuracy of 24% for the cross-validation procedure. The spatial pattern of the predicted soil
278 redistribution rates showed erosion in most of the catchment (Fig. 5). Only in grid cells with high flow
279 accumulation deposition occurred. The average redistribution rate from the grid cells (predY) amounted
280 to $-20.7 \text{ t ha}^{-1} \text{ yr}^{-1}$ (Fig 4d). Given the measured sediment yield at the outlet (Yield) of $-18.2 \text{ t ha}^{-1} \text{ yr}^{-1}$,
281 this corresponds to a 14% overestimation of soil loss by the Pu method (Fig 4d). The sediment yield
282 (Yield) corresponds to the off-site net erosion over time while the Pu-derived rates (siteY, meanY and
283 predY) to the on-site erosion over space. Their correspondence indicates that most of the on-site eroded
284 sediments are delivered to the outlet of the stream channel within the considered period.



285

286 Fig. 5 Soil redistribution rates assessed with Pu-derived soil redistribution rates (points) and spatial
287 prediction of soil redistribution rates based on these point rates using XY-coordinates, elevation and
288 flow accumulation as spatial covariates.

289 The Pu-derived soil erosion rates in the catchment were very high, with maximum values $<-40 \text{ t ha}^{-1} \text{ yr}^{-1}$
290 ¹. However, documented soil erosion peaks in this area can reach up to $100\text{--}150 \text{ t ha}^{-1} \text{ yr}^{-1}$ during
291 exceptional rainfall events (Porto et al., 2018; Porto et al., 2022). The sediment yield time series reveals
292 that besides the rainfall erosivity, particularly the second harvest of eucalyptus trees (1990), triggered
293 soil erosion. The soil conservation effect of the eucalyptus trees was also revealed by the lower Pu
294 inventory and, therefore, higher soil losses in the catchment area with scarce tree cover. The protective
295 effect of trees (Sorriso-Valvo et al., 1995; Zhou et al., 2002) and vegetation cover, in general, was also
296 found in other studies and reviewed by Zuazo and Pleguezuelo (2009). Flow accumulation, a proxy for
297 runoff concentration in a catchment, was an important predictor of soil erosion patterns. Interestingly,
298 the relationship was negative with lower soil losses and higher chances for deposition with increasing
299 flow accumulation. A reason for this was likely the collinearity between decreasing slopes with
300 increasing flow accumulation, reducing the sediment transport capacity (Xiao et al., 2017). Still, flow
301 accumulation performed better than alternative GAM models, including slope.

302 Mean Pu-239+240-based mean soil redistribution rates were $-20.7 \text{ t ha}^{-1} \text{ yr}^{-1}$ and 14% higher as
303 measured sediment yields at the catchment outlet. Given both methods' uncertainties and variability,
304 comparable magnitudes were achieved. In a recent study, Porto and Callegari (2022) found Cs-137
305 redistribution mean rates of $-20.4 \text{ t ha}^{-1} \text{ yr}^{-1}$. The Cs-137 and Pu-239+240 derived soil redistribution
306 rates are in good agreement.



307 **4 Conclusion**

308 Recent measurements of Pu-239+240 in a catchment in Southern Italy provided essential insights into
309 the suitability of the Pu-239+240 technique to estimate soil erosion rates. We also rigorously tested the
310 uncertainties involved in the approach. In our case study, the highest uncertainty resulted from the high
311 measurement uncertainty of low inventory samples, with a median CV of 21% and high measurement
312 uncertainty of <1% – 100%. This high uncertainty can, for future studies, be minimized by (i) taking
313 incremental soil depth samples, avoiding dilution with deeper horizons of low-activity soil and (ii)
314 extracting Pu on larger soil samples (~20g). Based on values with adequate measurement certainty, the
315 Pu-239-240 technique showed a low spatial variability of the reference inventory (CV <9%) and the
316 shape of the Pu distribution within the soil profile proved stable adsorption to the topsoil. Patterns of
317 inventory loss were related to soil redistribution processes, with the best spatial predictors being tree
318 cover and flow accumulation. The Pu-assessed redistribution rates were in agreement with Cs-137-
319 derived rates and sediment yield measurements at the catchment outlet.

320 Increasing climatic extremes associated with more intense farming practices endanger our soil
321 resources, and new tools to monitor soil losses are of utmost importance. So far, the tracer Cs-137 has
322 been a powerful approach to assess soil redistribution rates since its fallout. However, alternative tracers
323 are needed in light of the subsequent decay of Cs-137 approaching the detection limit. The Pu-239-240
324 technique works analogue to the Cs-137 technique. We conclude that Pu-239+240, with its considerably
325 longer half-life, is a suitable and promising soil redistribution tracer.

326



327 **Data availability**

328 The authors declare that all other data supporting the findings of this study are available within the
329 article and its Supplementary Information files.

330 **Acknowledgements**

331 We thank the University of Cadiz for the measurement of Pu-239+240 on the ICP-MS.

332 **Author information**

333 **Contributions**

334 K.M., C.A., and P. P. conceptualized the study. P.P. collected the samples, J.K.-W. measured them and
335 calculated the measurement uncertainties. K.M. and P.P. did the data analysis. K.M. wrote the
336 manuscript, and all co-authors contributed to the writing process.

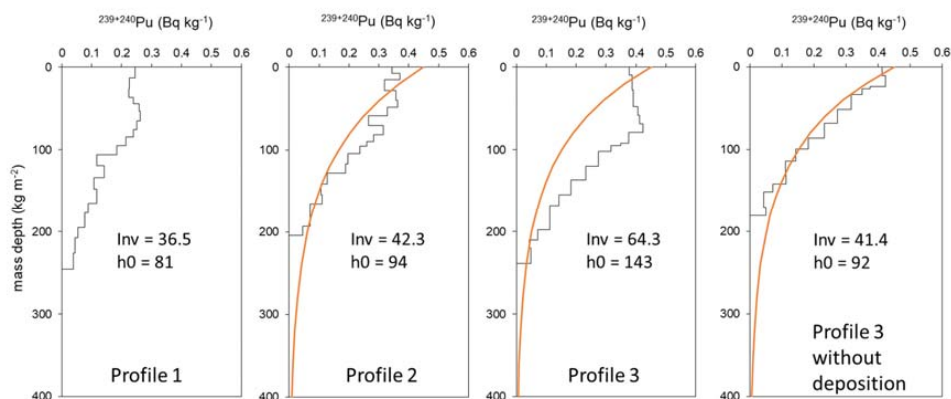
337 **Competing interests**

338 The authors declare no competing financial interests.

339



340 **Appendix**



341

342 Figure A1: Pu-239+240 activity with soil mass depth measured at three potential reference sites. Inv
343 corresponds to the total inventory of the soil, and h_0 to the shape factor of the exponential fit (orange).
344 Profile 3 was fitted with and without deposition layers. The standard deviation of the depth distribution
345 and h_0 factor of profiles 1, 2 and 3 (without deposition) was used for the uncertainty assessment in the
346 conversion model.

347



348 References

- 349 Alewell, C., Meusburger, K., Juretzko, G., Mabit, L., and Ketterer, M. E.: Suitability of $^{239+240}\text{Pu}$ and
350 ^{137}Cs as tracers for soil erosion assessment in mountain grasslands, *Chemosphere*, 103, 274–280,
351 10.1016/j.chemosphere.2013.12.016, 2014.
- 352 Alewell, C., Birkholz, A., Meusburger, K., Schindler Wildhaber, Y., and Mabit, L.: Quantitative
353 sediment source attribution with compound-specific isotope analysis in a C3 plant-dominated
354 catchment (central Switzerland), *Biogeosciences*, 13, 1587–1596, 10.5194/bg-13-1587-2016, 2016.
- 355 Alewell, C., Pitois, A., Meusburger, K., Ketterer, M., and Mabit, L.: $^{239+240}\text{Pu}$ from "contaminant" to
356 soil erosion tracer: Where do we stand?, *Earth-Science Reviews*, 172, 107–123,
357 10.1016/j.earscirev.2017.07.009, 2017.
- 358 Alewell, C., Ringeval, B., Ballabio, C., Robinson, D. A., Panagos, P., and Borrelli, P.: Global
359 phosphorus shortage will be aggravated by soil erosion, *Nature Communications*, 11, 4546,
360 10.1038/s41467-020-18326-7, 2020.
- 361 Amundson, R., Berhe, A. A., Hopmans, J. W., Olson, C., Sztein, A. E., and Sparks, D. L.: Soil and
362 human security in the 21st century, *Science*, 348, 6, 2015.
- 363 Arata, L., Alewell, C., Frenkel, E., A'Campo-Neuen, A., Iurian, A.-R., Ketterer, M. E., Mabit, L., and
364 Meusburger, K.: Modelling Deposition and Erosion rates with RadioNuclides (MODERN) – Part 2: A
365 comparison of different models to convert $^{239+240}\text{Pu}$ inventories into soil redistribution rates at
366 unploughed sites, *Journal of Environmental Radioactivity*, 162–163, 97–106,
367 <http://dx.doi.org/10.1016/j.jenvrad.2016.05.009>, 2016a.
- 368 Arata, L., Meusburger, K., Frenkel, E., A'Campo-Neuen, A., Iurian, A.-R., Ketterer, M. E., Mabit, L.,
369 and Alewell, C.: Modelling Deposition and Erosion rates with RadioNuclides (MODERN) – Part 1: A
370 new conversion model to derive soil redistribution rates from inventories of fallout radionuclides,
371 *Journal of Environmental Radioactivity*, 162–163, 45–55,
372 <http://dx.doi.org/10.1016/j.jenvrad.2016.05.008>, 2016b.
- 373 Avolio, S., Ciancio, O., Grinovero, C., Iovino, F., Mirabella, A., Raglione, M., Sfalanga, M., and Torri,
374 D.: Effetti del tipo di bosco sull'entità dell'erosione in unità idrologiche della Calabria—Modelli
375 erosivi, *Annali Istituto Sperimentale Selvicoltura*, 45–131 pp., 1980.
- 376 Borrelli, P., Robinson, D. A., Fleischer, L. R., Lugato, E., Ballabio, C., Alewell, C., Meusburger, K.,
377 Modugno, S., Schütt, B., Ferro, V., Bagarello, V., van Oost, K., Montanarella, L., and Panagos, P.: An
378 assessment of the global impact of 21st century land use change on soil erosion, *Nature*
379 *Communications*, 8, 2013, 10.1038/s41467-017-02142-7, 2017.
- 380 Cantore, V., Iovino, F., and Puglisi, S.: Influenza della forma di governo sui deflussi liquidi e solidi in
381 piantagioni di eucalitti, *L'Italia Forestale e Montana*, 5, 463–477, 1994.
- 382 Froehlich, M. B., Dietze, M. M. A., Tims, S. G., and Fifield, L. K.: A comparison of fallout U-236 and
383 Pu-239 uptake by Australian vegetation, *Journal of Environmental Radioactivity*, 151, 558–562,
384 10.1016/j.jenvrad.2015.06.021, 2016.
- 385 Hoo, W. T., Fifield, L. K., Tims, S. G., Fujioka, T., and Mueller, N.: Using fallout plutonium as a probe
386 for erosion assessment, *Journal of Environmental Radioactivity*, 102, 937–942,
387 10.1016/j.jenvrad.2010.06.010, 2011.
- 388 IAEA: Guidelines for using Fallout radionuclides to assess erosion and effectiveness of soil
389 conservation strategies, International Atomic Energy Agency, Vienna, Austria, 213, 2014.
- 390 Kato, H., Onda, Y., and Tanaka, Y.: Using Cs-137 and Pb-210(ex) measurements to estimate soil
391 redistribution rates on semi-arid grassland in Mongolia, *Geomorphology*, 114, 508–519,
392 10.1016/j.geomorph.2009.08.009, 2010.
- 393 Kelley, J. M., Bond, L. A., and Beasley, T. M.: Global distribution of Pu isotopes and ^{237}Np , *Science*
394 *of the Total Environment*, 237–238, 483–500, 10.1016/s0048-9697(99)00160-6, 1999.



- 395 Ketterer, M. E., Hafer, K. M., Link, C. L., Kolwaite, D., Wilson, J., and Mietelski, J. W.: Resolving
396 global versus local/regional Pu sources in the environment using sector ICP-MS, *Journal of Analytical*
397 *Atomic Spectrometry*, 19, 241-245, 10.1039/b302903d, 2004.
- 398 Ketterer, M. E., Zheng, J., and Yamada, M.: Applications of Transuranics as Tracers and Chronometers
399 in the Environment, *Handbook of Environmental Isotope Geochemistry*, Vols 1 and 2, edited by:
400 Baskaran, M., Springer-Verlag Berlin, Berlin, 395-417 pp., 2011.
- 401 Lal, R., Tims, S. G., Fifield, L. K., Wasson, R. J., and Howe, D.: Applicability of Pu-239 as a tracer for
402 soil erosion in the wet-dry tropics of northern Australia, *Nucl. Instrum. Methods Phys. Res. Sect. B-*
403 *Beam Interact. Mater. Atoms*, 294, 577-583, 10.1016/j.nimb.2012.07.041, 2013.
- 404 Lujanienė, G., Plukis, A., Kimtys, E., Remeikis, V., Jankunaite, D., and Ogorodnikov, B. I.: Study of
405 Cs-137, Sr-90, Pu-239, Pu-240, Pu-238 and Am-241 behavior in the Chernobyl soil, *Journal of*
406 *Radioanalytical and Nuclear Chemistry*, 251, 59-68, 10.1023/a:1015185011201, 2002.
- 407 Mabit, L., Benmansour, M., and Walling, D. E.: Comparative advantages and limitations of the fallout
408 radionuclides Cs-137, Pb-210(ex) and Be-7 for assessing soil erosion and sedimentation, *Journal of*
409 *Environmental Radioactivity*, 99, 1799-1807, 10.1016/j.jenvrad.2008.08.009, 2008.
- 410 Mabit, L., Benmansour, M., Abril, J. M., Walling, D. E., Meusburger, K., Iurian, A. R., Bernard, C.,
411 Tarján, S., Owens, P. N., Blake, W. H., and Alewell, C.: Fallout ²¹⁰Pb_{ex} as a soil and sediment tracer in
412 catchment sediment budget investigations: A review, *Earth-Science Reviews*, 138, 335-351, 2014.
- 413 Matisoff, G., Bonniwell, E. C., and Whiting, P. J.: Soil erosion and sediment sources in an Ohio
414 watershed using beryllium-7, cesium-137, and lead-210, *Journal of Environmental Quality*, 31, 54-61,
415 2002.
- 416 Meusburger, K., Mabit, L., Ketterer, M., Park, J.-H., Sandor, T., Porto, P., and Alewell, C.: A multi-
417 radionuclide approach to evaluate the suitability of Pu239+240 as soil erosion tracer, *Science of the*
418 *Total Environment*, 566, 1489-1499, 10.1016/j.scitotenv.2016.06.035, 2016.
- 419 Meusburger, K., Porto, P., Mabit, L., La Spada, C., Arata, L., and Alewell, C.: Excess Lead-210 and
420 Plutonium-239+240: Two suitable radiogenic soil erosion tracers for mountain grassland sites,
421 *Environmental Research*, 160, 195-202, 10.1016/j.envres.2017.09.020, 2018.
- 422 Meusburger, K., Evrard, O., Alewell, C., Borrelli, P., Cinelli, G., Ketterer, M., Mabit, L., Panagos, P.,
423 van Oost, K., and Ballabio, C.: Plutonium aided reconstruction of caesium atmospheric fallout in
424 European topsoils, *Sci Rep*, 10, 11858, 10.1038/s41598-020-68736-2, 2020.
- 425 Michelotti, E. A., Whicker, J. J., Eisele, W. F., Breshears, D. D., and Kirchner, T. B.: Modeling aeolian
426 transport of soil-bound plutonium: considering infrequent but normal environmental disturbances is
427 critical in estimating future dose, *Journal of Environmental Radioactivity*, 120, 73-80,
428 10.1016/j.jenvrad.2013.01.011, 2013.
- 429 Panagos, P., Imeson, A., Meusburger, K., Borrelli, P., Poesen, J., and Alewell, C.: Soil Conservation in
430 Europe: Wish or Reality?, *Land Degradation & Development*, 27, 1547-1551, 10.1002/ldr.2538, 2016.
- 431 Porto, P., Walling, D. E., and Ferro, V.: Validating the use of caesium-137 measurements to estimate
432 soil erosion rates in a small drainage basin in Calabria, Southern Italy, *Journal of Hydrology*, 248, 93-
433 108, 10.1016/s0022-1694(01)00389-4, 2001.
- 434 Porto, P., Walling, D. E., Ferro, V., and Di Stefano, C.: Validating erosion rate estimates provided by
435 caesium-137 measurements for two small forested catchments in Calabria, southern Italy, *Land*
436 *Degradation & Development*, 14, 389-408, 10.1002/ldr.561, 2003.
- 437 Porto, P., and Walling, D. E.: Validating the use of Cs-137 and Pb-210(ex) measurements to estimate
438 rates of soil loss from cultivated land in southern Italy, *Journal of Environmental Radioactivity*, 106,
439 47-57, 10.1016/j.jenvrad.2011.11.005, 2012.
- 440 Porto, P., Walling, D. E., and Callegari, G.: Using ¹³⁷Cs and ²¹⁰Pb_{ex} measurements to investigate the
441 sediment budget of a small forested catchment in southern Italy, *Hydrological Processes*, 27, 795-806,
442 10.1002/hyp.9471, 2013.



- 443 Porto, P., Walling, D. E., Alewell, C., Callegari, G., Mabit, L., Mallimo, N., Meusburger, K., and
444 Zehring, M.: Use of a ^{137}Cs re-sampling technique to investigate temporal changes in soil erosion and
445 sediment mobilization for a small forested catchment in southern Italy, *Journal of Environmental*
446 *Radioactivity*, 138, 137-148, 2014.
- 447 Porto, P., Cogliandro, V., and Callegari, G.: Exploring the performance of the SEDD model to predict
448 sediment yield in eucalyptus plantations. Long-term results from an experimental catchment in
449 Southern Italy, *IOP Conference Series: Earth and Environmental Science*, 107, 012020, 10.1088/1755-
450 1315/107/1/012020, 2018.
- 451 Porto, P., Bacchi, M., Preiti, G., Romeo, M., and Monti, M.: Combining plot measurements and a
452 calibrated RUSLE model to investigate recent changes in soil erosion in upland areas in Southern Italy,
453 *J. Soils Sediments*, 22, 1010-1022, 10.1007/s11368-021-03119-2, 2022.
- 454 Porto, P., and Callegari, G.: Comparing long-term observations of sediment yield with estimates of soil
455 erosion rate based on recent Cs-137 measurements. Results from an experimental catchment in Southern
456 Italy, *Hydrological Processes*, 36, 10.1002/hyp.14663, 2022.
- 457 Qiao, J. X., Hansen, V., Hou, X. L., Aldahan, A., and Possnert, G.: Speciation analysis of I-129, Cs-
458 137, Th-232, U-238, Pu-239 and Pu-240 in environmental soil and sediment, *Applied Radiation and*
459 *Isotopes*, 70, 1698-1708, 10.1016/j.apradiso.2012.04.006, 2012.
- 460 Reichstein, M., Bahn, M., Ciais, P., Frank, D., Mahecha, M. D., Seneviratne, S. I., Zscheischler, J.,
461 Beer, C., Buchmann, N., Frank, D. C., Papale, D., Rammig, A., Smith, P., Thonicke, K., van der Velde,
462 M., Vicca, S., Walz, A., and Wattenbach, M.: Climate extremes and the carbon cycle, *Nature*, 500, 287-
463 295, 10.1038/nature12350, 2013.
- 464 Schimmack, W., Auerswald, K., and Bunzl, K.: Can $\text{Pu}^{239+240}$ replace Cs-137 as an erosion tracer in
465 agricultural landscapes contaminated with Chernobyl fallout?, *Journal of Environmental Radioactivity*,
466 53, 41-57, 10.1016/S0265-931X(00)00117-X, 2001.
- 467 Sorriso-Valvo, M., Bryan, R. B., Yair, A., Iovino, F., and Antronico, L.: Impact of afforestation on
468 hydrological response and sediment production in a small Calabrian catchment, *CATENA*, 25, 89-104,
469 [https://doi.org/10.1016/0341-8162\(95\)00002-A](https://doi.org/10.1016/0341-8162(95)00002-A), 1995.
- 470 Teramage, M. T., Onda, Y., Wakiyama, Y., Kato, H., Kanda, T., and Tamura, K.: Atmospheric Pb-210
471 as a tracer for soil organic carbon transport in a coniferous forest, *Environ. Sci.-Process Impacts*, 17,
472 110-119, 10.1039/c4em00402g, 2015.
- 473 Tims, S. G., Everett, S. E., Fifield, L. K., Hancock, G. J., and Bartley, R.: Plutonium as a tracer of soil
474 and sediment movement in the Herbert River, Australia, *Nucl. Instrum. Methods Phys. Res. Sect. B-*
475 *Beam Interact. Mater. Atoms*, 268, 1150-1154, 10.1016/j.nimb.2009.10.121, 2010.
- 476 Wallbrink, P. J., and Murray, A. S.: Determining soil loss using the inventory ratio of excess lead-210
477 to cesium-137, *Soil Science Society of America Journal*, 60, 1201-1208, 1996.
- 478 Walling, D. E., He, Q., and Appleby, P. G.: Conversion models for use in soil-erosion, soil-
479 redistribution and sedimentation investigations, in: *Handbook for the Assessment of Soil Erosion and*
480 *Sedimentation using Environmental Radionuclides*, edited by: Zapata, F., The Netherlands, 111-164,
481 2002.
- 482 Walling, D. E., Zhang, Y., and He, Q.: Conversion models and related software, in: *Guidelines for*
483 *Using Fallout Radionuclides to Assess Erosion and Effectiveness of Soil Conservation Strategies*,
484 *IAEA-TECDOC-1741*, Vienna, 125-148, 2014.
- 485 Wilken, F., Fiener, P., Ketterer, M., Meusburger, K., Muhindo, D. I., van Oost, K., and Doetterl, S.:
486 Assessing soil redistribution of forest and cropland sites in wet tropical Africa using $^{239+240}\text{Pu}$ fallout
487 radionuclides, *SOIL*, 7, 399-414, 10.5194/soil-7-399-2021, 2021.
- 488 Wood, S. N.: Low-rank scale-invariant tensor product smooths for generalized additive mixed models,
489 *Biometrics*, 62, 1025-1036, 10.1111/j.1541-0420.2006.00574.x, 2006.



- 490 Xiao, H., Liu, G., Liu, P., Zheng, F., Zhang, J., and Hu, F.: Sediment transport capacity of concentrated
491 flows on steep loessial slope with erodible beds, *Sci Rep*, 7, 2350, 10.1038/s41598-017-02565-8, 2017.
- 492 Xu, Y., Pan, S., Wu, M., Zhang, K., and Hao, Y.: Association of Plutonium isotopes with natural soil
493 particles of different size and comparison with ¹³⁷Cs, *Science of The Total Environment*, 581-582,
494 541-549, <https://doi.org/10.1016/j.scitotenv.2016.12.162>, 2017.
- 495 Xu, Y. H., Qiao, J. X., Hou, X. L., and Pan, S. M.: Plutonium in Soils from Northeast China and Its
496 Potential Application for Evaluation of Soil Erosion, *Sci Rep*, 3, 10.1038/srep03506, 2013.
- 497 Xu, Y. H., Qiao, J. X., Pan, S. M., Hou, X. L., Roos, P., and Cao, L. G.: Plutonium as a tracer for soil
498 erosion assessment in northeast China, *Science of the Total Environment*, 511, 176-185,
499 10.1016/j.scitotenv.2014.12.006, 2015.
- 500 Zapata, F.: The use of environmental radionuclides as tracers in soil erosion and sedimentation
501 investigations: recent advances and future developments, *Soil & Tillage Research*, 69, 3-13, 2003.
- 502 Zhou, G. Y., Morris, J. D., Yan, J. H., Yu, Z. Y., and Peng, S. L.: Hydrological impacts of reforestation
503 with eucalypts and indigenous species: a case study in southern China, *Forest Ecology and
504 Management*, 167, 209-222, [https://doi.org/10.1016/S0378-1127\(01\)00694-6](https://doi.org/10.1016/S0378-1127(01)00694-6), 2002.
- 505 Zuazo, V. c. H. D., and Pleguezuelo, C. R. o. R.: Soil-Erosion and Runoff Prevention by Plant Covers:
506 A Review, in: *Sustainable Agriculture*, edited by: Lichtfouse, E., Navarrete, M., Debaeke, P.,
507 Véronique, S., and Alberola, C., Springer Netherlands, Dordrecht, 785-811, 2009.
- 508